CrossMark

Effect of Nozzle Exit Turbulence on the Column Trajectory and Breakup Location of a Transverse Liquid Jet in a Gaseous Flow

Mohsen Broumand[1] · Graham Rigby[1] · Madjid Birouk[1]

Abstract This study examines the effect of fully developed turbulent flow at the exit of nozzle/injector on the trajectory and column breakup location of a liquid jet injected transverly into a gaseous crossflow. Liquid jet trajectory and column breakup for different nozzle geometries at different velocities of liquid jet and crossflow are analytically and experimentally Investigated. Shadowgraph imaging technique is used to determine the jet trajectory and breakup location of a transverse liquid jet in a uniform airflow. Particle image velocimetry (PIV) is used to measure the near-field velocity profile of a liquid jet discgarged into a quiescent atmosphere. The experimental results show a higher penetration and breakup height for the liquid jet ensuing from a nozzle with a smaller length to diameter ratio. This is due to the surface irregularities of the liquid column of a turbulent jet, which breaks up and consequently follows the cross airflow sooner. In order to capture the effect of turbulence, the analytical trajectory correlation developed in our previous studies is modified to account for the discharge coefficient of a nozzle. The discharge coefficient is estimated indirectly by comparing the liquid column trajectory predicted by the modified analytical correlation with that determined experimentally. The indirectly determined discharge coefficient is then used in the analytical correlation for predicting the breakup height of a transverse liquid jet. The results predicted using this approach are in good agreement with the experimental data of the present study at standard temperature and pressure (STP) test conditions.

Keywords Liquid jet · Cross airflow · Jet trajectory · Breakup location · Discharge coefficient · Nozzle geometry

---

✉ Madjid Birouk
madjid.birouk@umanitoba.ca

[1] Department of Mechanical Engineering, University of Manitoba, Winnipeg, Manitoba, R3T 5V6, Canada

Nomenclature

A_o	nozzle exit area, m^2
Bo	Bond number, $\rho_l g d_j^2 / \sigma$
C_D	liquid column average drag coefficient
C_d	discharge coefficient of nozzle
d_j	liquid jet diameter at the nozzle exit, m
L	exit length of nozzle, m
$\dot{m}_f$	nozzle mass flowrate, kg/s
q	jet momentum flux ratio, $\rho_l v_j^2 / \rho_g u_g^2$
Re_j	jet Reynolds number, $\rho_l v_j d_j / \mu_l$
t_b	column breakup time, s
t_i	onset of surface breakup time, s
t_s	characteristic liquid-phase time, $\left(\rho_l / \rho_g \right)^{\frac{1}{2}} d_j / u_g$
t_v^*	characteristics viscous time, $d_j^2 / (\mu_l / \rho_l)$
u_g	crossflow velocity, m/s
v_j	liquid velocity at the nozzle exit, m/s
We_g	gas phase Weber number, $\rho_g u_g^2 d_j / \sigma$
We_j	jet Weber number $\rho_l v_j^2 d_j / \sigma$
x	coordinate in gas crossflow (horizontal) direction , m
z	coordinate in liquid injection (vertical) direction, m

Greek symbol

μ	viscosity, kg/(m.s)
ρ	density, kg/m^3
σ	liquid surface tension, N/m
ψ_o	injection angle

Subscripts

b	column breakup
g	gas
j	jet
l	liquid
w	water

1 Introduction

The flowfield associated with a liquid jet injected transversely into a subsonic gaseous crossflow, known as a transverse liquid jet, has superior mixing properties compared to a jet in quiescent surroundings, which makes this flowfield layout appealing especially for engineering applications when rapid mixing is desired [1, 2]. This flowfield has various applications in power generation systems from stationary to avionic combustion engines, such as low NOx gas turbines, lean premixed prevaporized (LPP) combustors, high speed direct injection (HSDI) diesel engines and aircraft engine afterburner sections. The application of this flowfield configuration in these power systems is advantageous as it enhances liquid fuel-air mixture, which in turn improves flame stabilization, fuel conversion efficiency, and accordingly emissions reduction [3, 4]. Another application of transverse liquid jet is the injection of lubricating oil into a rotating annular airflow in the cavity of

aero-engine bearing chamber [5, 6]. The injection of suspension/liquid radially into a jet flame during thermal spray processes is also another example of the application of this flowfield configuration [7].

When a liquid jet is injected transversely into a subsonic gaseous crossflow, it leaves the injector/nozzle as an unbroken column, begins to ruffle as a result of axial instabilities which develop along the liquid column, and finally breaks up into ligaments and droplets. This process is named as the column breakup process [8–10]. As liquid begins to disintegrate from the surface of the liquid column (as a result of hydrodynamic instabilities on the jet lateral surface), the surface breakup process becomes dominant [8–10]. In the breakup process of a transverse liquid jet, both column and surface breakup mechanisms coexist but with the predominance of one over the other depending on flow conditions. Liquid fragments (i.e., ligaments and droplets) shedding from a jet along its trajectory undergo subsequent secondary breakup process leading to smaller droplets, and consequently the formation of a spray. As is illustrated in Fig. 1, the core of a transverse liquid jet (i.e., liquid column) forms a continuous stream between the jet exit and the location of its complete fracture, and it is referred to as the column breakup location. Data describing the column trajectory and breakup location of a transverse liquid jet is important for the design of the aforementioned power systems. For instance, this information is needed to prevent liquid impingement onto a combustor's wall. More importantly, these features are necessary for predicting liquid distribution which directly affects droplets primary and secondary breakup, droplets collision, evaporation and vapor mixing rate with the gaseous phase, and thereby affects the overall efficiency of a system. Nonetheless, accurate acquisition of these features is difficult experimentally because of droplets density around the near-field liquid column [11, 12].

Numerous studies examined the role of different parameters which include liquid properties, test conditions, and liquid injector/nozzle geometry on the column trajectory and breakup location of a transverse liquid jet (e.g., [14] and references cited therein). Generally, it is revealed that jet momentum flux ratio, $q = \rho_l v_j^2 / \rho_g u_g^2$, plays the most important parameter for predicting the column trajectory and breakup height, z_b/d_j, of a transverse liquid jet.
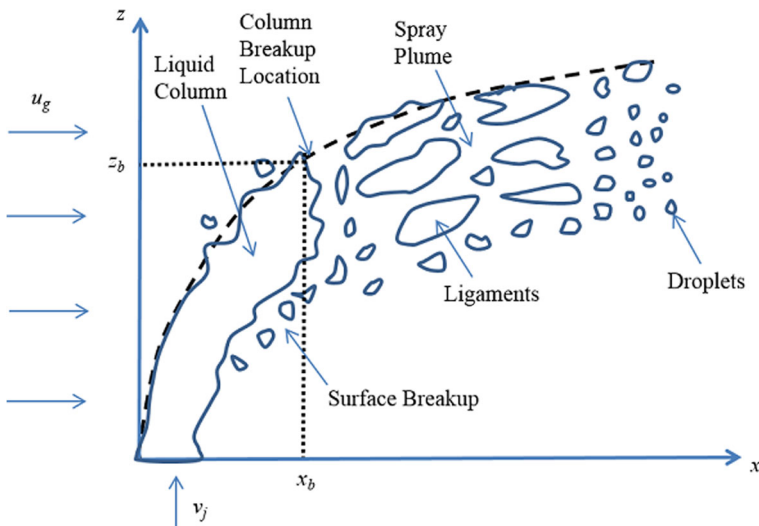

Fig. 1 Schematic diagram of a liquid jet injected perpendicularly into a gaseous crossflow. Reprinted from Ref. [13] with permission from Begell House

Conversely, the column breakup distance, x_b/d_j, is found to be a constant value. However, there exist differences in the predictions of these jet features between different published correlations, even at constant q. The reason for these discrepencies can be attributed to different factors such as the variation in liquid properties, test conditions and nozzle internal geometries, as well as errors associated with measurement and numerical uncertainties [13, 14]. For instance, q appears and plays a key role in all publsihed correlations for predicting a liquid jet's trajectory and breakup location. However, this parameter depends on the value of liquid jet velocity, v_j. Thus the reliability of q strongly depends on that of v_j. It appeared that in most published correlations, v_j is calculated based on the volumetric flow rate divided by the injector (or nozzle) orifice cross sectional area, which implies a unity value of the discharge coefficient [15]. The actual jet velocity is inversely proportional to the discarge coefficient of an injector/nozzle, C_d. This coefficient, C_d, is a function of several factors such as nozzle (or injector) internal geometry, liquid injection pressure, jet Reynolds number (Re_j), turbulence, cavitation and hydraulic flip, ambient pressure, etc. [16]. Consequently, each of these parameters can affect the actual value of v_j and hence q, which in turn can result in different predictions of the column trajectory and its breakup location.

Brown et al. [15, 17, 18] reported that the value of C_d depends on both the internal geometry and diameter of a nozzle which can change the value of the momentum flux ratio, q, up to 50% for a nozzle with a length to diameter ratio of $L/d_j = 4$. To address this issue, they considered a non-unity C_d of a nozzle by taking into account the nozzle's injection pressure instead of v_j, and proposed a trajectory correlation with different set of coefficients for each specific nozzle [17]. Ahn et al. [19, 20] investigated the effect of cavitation and hydraulic flip on C_d and reported that the liquid column trajectory of non-cavitating and cavitating jets have a similar trend, but were different than that of jets which experience hydraulic flip as this causes liquid jet flow to detach from the inner wall of the orifice. They also asserted that the liquid breakup height and distance of a cavitating flow is smaller in comparison with that of a non-cavitating jet. Lubarsky et al. [21] investigated the trajectory of Jet-A fuel injected into a cross airflow using different injector geometries (i.e., sharp edge with $L/d_j = 10$, and round edge with $L/d_j \sim 1$). They reported that, within their tested range of Re_j, the discharge coefficient of a sharp edge orifice is relatively constant, $C_d \sim 0.75$; while the discharge coefficient of a round edge orifice is $C_d \sim 0.96$ for Reynolds numbers exceeding $Re_j = 10,000$. They indicated a greater spray penetration into a cross airflow ($\sim 12\%$) for a sharp edge orifice compared to a round edged orifice.

Lee et al. [22] investigated the deformation and breakup properties of a turbulent liquid jet in a gaseous crossflow. They asserted that the presence of turbulence in a liquid jet has little effect on liquid column trajectory but exerted an apparent impact on the column breakup loction; that is, $x_b/d_j = 5.20$ and $x_b/d_j = 8.64$ for turbulent and nonturbulent liquid jet in a crossflow, respectively. Osta et al. [23] measured the column breakup distance of a turbulent liquid jet issuing from nozzles with different length/diameter ratios. They showed that the column breakup distance of a turbulent liquid jet with different length/diameter ratios ranged between the two constant values in agreement with the findings of Lee et al. [22] for turbulent liquid jet, and Sallam et al. [24] for nonturbulent liquid jets; i.e., $x_b/d_j = 5.20-8$. Osta et al. [23] also measured the column breakup height of a turbulent liquid jet by testing nozzles with different length/diameter ratios, and proposed an empirical correlation for each specific length/diameter ratio, which is expressed as follows: $z_b/d_j = 3.3q^{0.50}$ for a length/diameter ratio of 10 and $d_j = 4\ mm$, $z_b/d_j = 3.1q^{0.5}$ for a length/diameter ratio of 20 and $d_j = 2\ mm$, $z_b/d_j = 2.7q^{0.5}$ for a length/diameter ratio of 40 and $d_j = 4\ mm$.

To examine the effect of jet exit turbulence on the column trajectory and breakup location of a transverse liquid jet, the spray regime map provided by Wu et al. [25] for round liquid

jets injected into a quiescent gaseous environment (see Fig. 2) is utilized. According to this map, liquid jet has a smooth surface with no reattachment (i.e., implying a non-turbulent flow) for a nozzle's length/diameter ratio less than 4–6 at high Re_j. On the other hand, a nozzle with a larger length/diameter ratio generates a fully developed turbulent flow at the jet exit for sufficiently high Re_j.

Furthermore, in order to assess the impact of jet exit turbulence conditions on the characteristics of a liquid jet injected into a gaseous crossflow, details of the geometries and the range of Re_j associated with different studies (e.g., References [9, 21–23, 26, 27]) on the transverse liquid jets are added in Fig. 2. As it is shown in this figure, the type of nozzles used in different experiments is either under the range of $L/d_j = 4 - 6$ or above this line, and there exists no study that examined the rang of nozzles on both (i.e., lower and upper) side of this line except Lubarsky et al. [21]. In their study [21], however, the shape of nozzles are different, and they focused on a comparison between the trajectory of a transverse liquid jet injected from a sharp edge orifice versus a round edged orifice. This indicates that the effect of jet exit conditions has not yet been examined. In fact, the impact of nozzle exit conditions, particularly that of turbulence which could be one of the probable reasons of the discrepancies between the correlations proposed for liquid column trajectory and its breakup location, seems to be ignored.

The present study, therefore, aims at examining the role of fully developed turbulent flow conditions at the nozzle exit on the predictions of the trajectory and column breakup location of a transverse liquid jet when q and other controlling nondimensional parameters are kept unchanged. To do so, three round edged nozzles with a diameter of $d_j = 2$ mm and
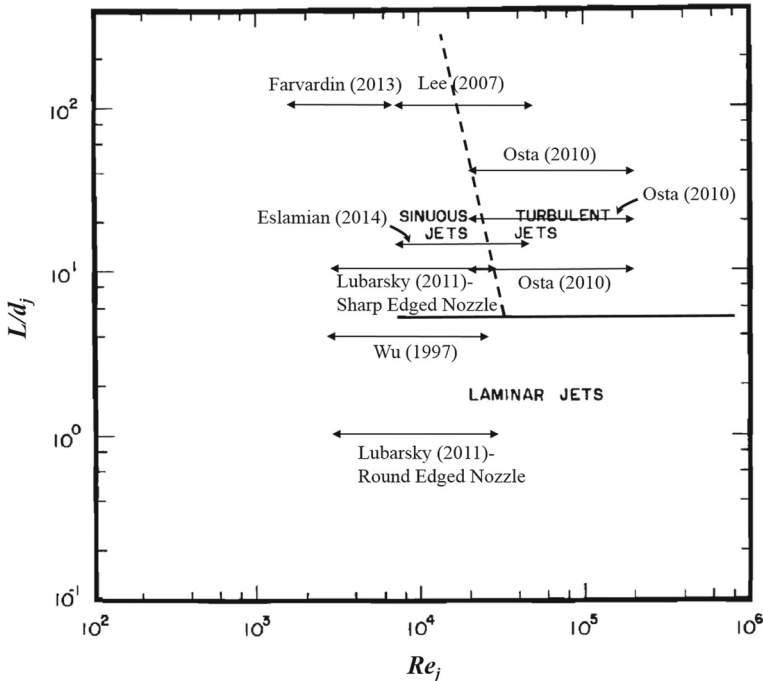

Fig. 2 Primary breakup regime map for round liquid jets injected into quiescent gases Adapted by the present authors from Ref. [25] with permission from Begell House

$L/d_j = 4, 20$ and 40 are used at a sufficiently high range of $Re_j = 17 \times 10^3 - 57 \times 10^3$ (in order to examine the effect of fully developed turbulent exit conditions). The mean axial velocity profiles and axial turbulence intensity at a region very close to (near-field) the nozzle exit are obtained using a PIV, and the column trajectory and its breakup location are extracted from shadowgraphy images. The correlation for predicting liquid jet column trajectory, which was developed in our previous studies [28, 29], with unknown discharge coefficient, C_d, is compared with the present experimental data in order to estimate the value of C_d for each specific nozzle geometry at different test conditions. Based on the obtained values of C_d, the analytical correlation for predicting the column breakup height is used to predict these jet characteristics for both non-turbulent and turbulent liquid jet at standard temperature and pressure (STP) test conditions.

2 Methodology

Both analytical and experimental approaches, which will be described in the following subsections, are employed to examine the nozzle exit turbulence on the prediction of the trajectory of a liquid jet and its breakup length.

2.1 Analytical method

For predicting the trajectory of a liquid jet injected perpendicularly into a subsonic cross airflow, the sinusoidal-exponential correlation proposed by Broumand and Birouk [29] has the following form:

$$\frac{z}{d_j} = \frac{\beta}{\alpha} \left(\sin^{-1} \left[\sin \psi_o . exp \left(\left(\frac{\alpha}{\beta} \right) \frac{x}{d_j} \right) \right] - \psi_o \right) \qquad (1)$$

where $\psi_o = \pi/2$ is the injection angle, and d_j is the liquid jet diameter at the nozzle exit. β, α and γ are the coefficients which are dependent on different non-dimensional numbers and their modified forms are presented below. In the present study, two modifications are performed to estimate the coefficients in Eq. 1. In order to make the liquid injection velocity independent of the nozzle's internal geometry and Re_j (i.e., nozzle exit conditions) and deteremine the actual jet velocity needed for calculating q, Re_j, and We_j, the nominal jet velocity, $v_{j,nom}$, which is calculated based on the metered liquid flowrate divided by the nozzle exit area (i.e., $C_d = 1$), is instead normalized by the actual nozzle's discharge coefficient (non-inity discharge coefficient; i.e., $C_d \neq 1$). The discharge coefficient of a plain-orifice atomizer/nozzle can be expressed as follows [16]:

$$v_{j,act} = \frac{\dot{m}_f}{\rho_l A_o C_d} = \frac{v_{j,nom}}{C_d} \qquad (2)$$

Equation 1 uses an average value of the discharge coefficient suggested by Brown et al. [15] with some degree of uncertainty. Thus, in order to improve the reliability of Eq. 1, a more accurate value of the discharge coefficient of each specific nozzle must be determined. In doing so, the ligaments and droplets formed by the surface breakup mechanism are assumed to leave the liquid column from its downstream half [22, 24], as opposed to droplets formation over the entire periphery of a liquid jet in a quiescent gaseous environment [30]. Hence, the mass ratio used for calculating the rate of mass shedding from the liquid column in Eq. 1 is halved (as indicated in the second term of Eq. 5). Given the

two afornmentioned assumptions, the coefficients of Eq. 1 can be rewritten explicitly as a function of C_d. They are expressed as follows:

$$\beta = \frac{2C_d^2}{We_j} - 1 \tag{3}$$

$$\alpha = \gamma + \left(\frac{Bo.C_d^2}{We_j}\right)^2 \frac{1}{\gamma} \tag{4}$$

$$\gamma = \frac{2C_D.C_d^2}{\pi q} + \frac{1}{2}\left[\left(\frac{410C_d^2}{q}\right)^{\frac{3}{4}}\left(\frac{\rho_g}{\rho_l}\right)^{-\frac{1}{12}}\left(\frac{\mu_g}{\mu_l}\right)^{\frac{1}{6}}\left(\frac{Re_j}{C_d}\right)^{-\frac{1}{2}}\left(\frac{t_b - t_i}{t_b}\right)\right] \tag{5}$$

where $q = \rho_l v_j^2/\rho_g u_g^2$, $Re_j = \rho_l v_j d_j/\mu_l$, and $We_j = \rho_l v_j^2 d_j/\sigma$ are simply calculated based on the nominal jet velocity, $v_{j,nom}$, and the Bond number is defined as $Bo = \rho_l g d_j^2/\sigma$. An average value of the drag coefficient, C_D, along the entire length of the liquid column for different liquids is adopted from the correlation proposed by Wu et al. [9] as $C_D/C_{Dw} = 0.984(\mu_l/\mu_w)^{0.364}$, where $C_{Dw} = 1.51$ and μ_w are the water drag coefficient and viscosity, respectively. The column breakup time, t_b, is adopted from Sallam et al. [24] for $We_g < 300$ as $t_b = 2.5t_s$, where $t_s = \left(\rho_l/\rho_g\right)^{\frac{1}{2}} d_j/u_g$ is the characteristic liquid-phase time, and the time of the onset of surface breakup, t_i, is defined as $t_i = 0.0004\left[\left(\mu_l/\mu_g\right)/We_g\right]t_v^*$, where $t_v^* = d_j^2/(\mu_l\rho_l)$ is the characteristic viscous time.

The column breakup height, z_b/d_j (i.e., liquid jet streamwise direction), is predicted following the approach of Wu et al. [9], who assumed that the time required for the column to breakup is a fixed portion of the characteristic liquid-phase time, $t_b = C_z t_s$. Assuming a constant liquid jet velocity, v_j, up to the column breakup location, the column breakup height, z_b, can be obtained by multipliying t_b by v_j. Then, using $t_b = C_z t_s$ and the definition of $t_s = \left(\rho_l/\rho_g\right)^{\frac{1}{2}} d_j/u_g$, and also employing Eq. 2, the correlation for prediciting the column breakup height can be expressed as follows:

$$\frac{z_b}{d_j} = C_z\left[\frac{q}{C_d^2}\right]^{\frac{1}{2}} \tag{6}$$

where q is calculated based on the nominal jet velocity, $v_{j,nom}$, and C_z was adopted from Sallam et al. [24] as $C_z = 2.5$ for $We_g < 300$. The column breakup distance, x_b/d_j (i.e., cross airflow streamwise direction), as discussed by Wu et al. [9], should be relatively independent of q due to the cancellation of aerodynamic effect on the liquid acceleration and on the column breakup time scale. Hence, it can be represented by a constant as $x_b/d_j = C_x$.

Exploiting these two modified correlations for the column trajectory, Eq. 1, and its breakup location, Eq. 6, which are explicitly expressed as a function of C_d, the impact of nozzle exit turbulence can be captured and predicted quantitatively.

2.2 Experimental method

2.3 Test apparatus and conditions

The experimental apparatus is an open wind tunnel which operates at atmospheric conditions and generates a uniform crosswind (crossflow) in a transparent test section made of acrylic. Several honeycomb and screens are utilized immediately before the test section to remove lateral and swirl velocity components in the test section. The test section has a

square cross-section of 305 mm × 305 mm and a length of 600 mm. The blower generating the wind/flow in the tunnel is controlled by a frequency drive, and the full characterization of flow in the test section versus different blower's speed has been performed using laser Doppler velocimetry (LDV) and reported in our previous publications (e.g., Iyogun et al. [31], Birouk et al. [32, 33]). The wind tunnel is capable of generating a uniform flow in the test section with a velocity ranging between 7.5 m/s and 70.7 m/s [22, 31, 33]. The nozzle is setup flush with the inner surface of the test section.

An injection system is used to deliver the liquid fluid into the test section through a nozzle which is located 200 mm downstream of the inlet of the test section. It consists of a compressed nitrogen tank which supplies high pressure nitrogen into a sealed chamber which contains the working fluid. The working fluid is introduced to the sealed chamber via either a liquid storage tank in the case of water or via a handheld funnel for other liquids. The liquid in the chamber is pressurized to cause liquid to flow out of the bottom of the chamber into a supply tubing and finally discharges through a nozzle into the test section. The pressure in the chamber is controlled by a typical mechanical pressure regulator attached to the nitrogen tank. The pressure in the chamber is measured using a digital pressure gauge having an output reading in $psig$ with a single decimal digit on a refresh rate of approximately 1 Hz. The pressure gauge assembly includes a manually opened release valve to lower the chamber pressure, as well as a safety release valve which opens automatically at a chamber pressure of approximately 140 $psig$. More detail about the setup can be found in [34, 35].

Three different nozzle geometries with two different types of contraction profiles are used in the experiment (see Fig. 3). The two different contractions have a conical section with 60° where there is no gradual change in the cross-section, and a rounded one which has a 2 mm radius edge fillet around the exit diameter. All of these nozzles are manufactured out of stainless steel rods with an outer diameter of 9.5 mm. The internal cross-section of all nozzles is circular with a diameter of $d_j = 2$ mm. The nozzle specifications are tabulated in Table 1.

Each nozzle has been calibrated to determine the relationship between chamber pressure and nozzle exit velocity. The liquid jet nominal velocity is calculated based on the volume flow rate divided by the nozzle's cross sectional area.
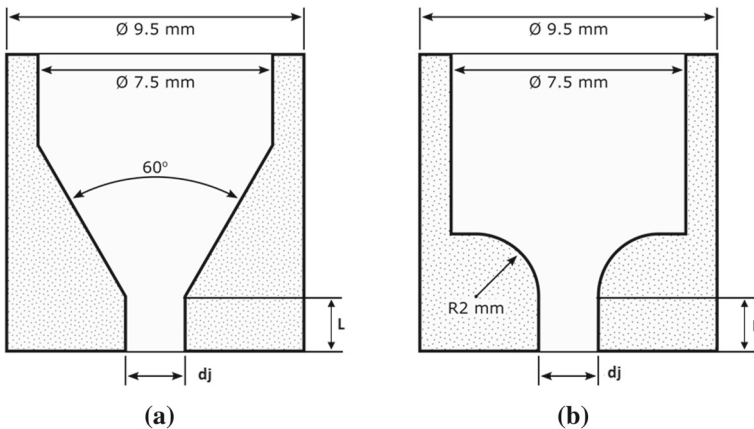

Fig. 3 Schematic of the different nozzles: **a**) Nozzle N (i-iii) with 60° contraction, and (**b**) N (4) and N (2) with rounded contraction

Table 1 Geometric parameters of the nozzles used in the experiment

Nozzle Name	Contraction Type	L(mm)	$d_j(mm)$	L/d_j
N(i-iii)	60° (L/d_j)	8	2	4
N4	Round (large L/d_j)	40	2	20
N2	Round (large L/d_j)	80	2	40

2.4 Imaging setup

Shadography technique is employed to image the jet trajectory and its breakup location, while particle image velocimetry (PIV) is used to measure the liquid jet axial mean velocity and its corresponding axial turbulence intensity at distances very close to the nozzle exit.

Imaging of a liquid jet in the a crossflow is performed in the near- and far-field. In the near-field imaging, the camera is setup close to the test section to reveal details when the liquid jet first comes into contact with the crossflow. These images divulge the interaction between the jet's surface and crossflow at distances very close to the nozzle exit which would influence the overall jet trajectory and breakup location.

The imaging of the far-field seeks to determine the overall trajectory of the injected liquid jet and the column breakup location. For both the near- and far-field imaging of the liquid jet in the crossflow, 75 images are collected using a high-speed camera with an exposure time of 5 μs and a frame rate of 30 fps with a resolution of 1280×1024 pixels. However, for the far-field, the camera is setup much farther back from the test section in order to image a much larger area. In order to improve the uniformity of the light source, the light is reflected off a spherical concave mirror which has a focal point on the camera's sensor. This setup is schematically illustrated in Fig. 4.

The liquid jet upwind boundary is used to determine the column trajectory in the crossflow. The jet's trajectory is determined by averaging 75 images using an in-house developed MATLAB code. A threshold has been applied to these images to identify the jet/spray boundary [17, 36]. Following the method of Thawley et al. [37], the breakup length of the liquid jet is defined as the point where the liquid column first separates. For each test conditions, the breakup location of 10 successive images is first identified manually, and an average value is used to define the breakup location in the crossflow and liquid jet streamwise direction. The uncertainty in the average for the breakup hight is found less than $1 \times d_j$.
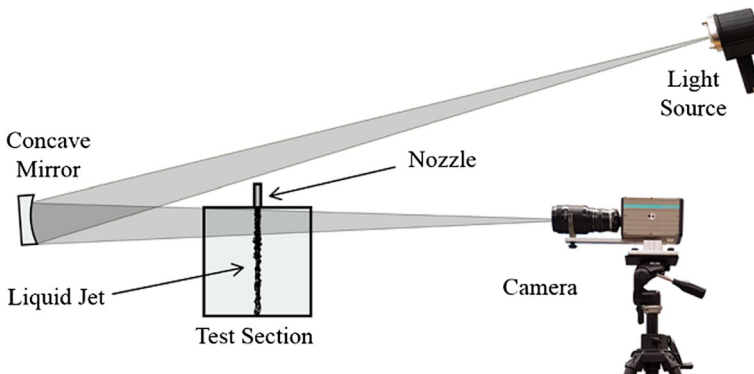

Fig. 4 Schematic of the imaging system of liquid jet injected into a crossairflow

A Dantec Dynamics Particle Image Velocimetry (PIV) is used to measure the axial mean velocity and its corresponding turbulence intensity of liquid jet in a quiescent atmosphere (without crossflow). The PIV setup consists of a Nd:YAG laser with a pulse energy of 135 mJ and a repetition rate of 10 Hz, a double-frame FlowSense EO 4M CCD camera with 20.4 fps at 2048×2048 pixel^2 sensor resolution, and Dynamic Studio Software. Silver-coated hollow glass spheres of 10 μm are used as seeding particles for the liquid jet. The duration between the two pulses is adjusted according to the jet velocity which ranges between 2–4 μs. Twelve hundred image pairs are acquired in a field of view of 24×24 mm^2. An interrogation area of 32×32 with 50% overlap in addition to range validation for spurious vectors elimination are applied in post processing. An average filter of 3×3 vectors is used for flow field smoothing.

3 Results and Discussion

3.1 Liquid jet visualization and measurements

To investigate the effect of the presence of turbulence at the nozzle exit on the trajectory and breakup location of a transverse liquid jet, several experiments were carried out using different nozzle geometries and test conditions. Conditions for the appearance of non-turbulent and turbulent round liquid jet were obtained from the primary breakup regime map proposed by Wu et al. [25], as indicated in Fig. 2. Two different sets of nozzles (small: $L/d_j = 4$, and large: $L/d_j = 20$ and 40 to reach a fully developed turbulent flow) with similar nozzle exit diameter, $d_j = 2\,mm$, were employed.

As is qualitatively illustrated in Fig. 5, the shadowgraph images show that, in the near-field region (up to $z_b/d_j \approx 12$), the column surface of the liquid jet issuing from a larger length/diameter ratio (Fig. 5b) exhibits more surface irregularities and produces more ligaments particularly at the upwind side of the column (i.e., where crossflow is from right to left) than its counterpart's smaller length/diameter ratio nozzle (Fig. 5a). The relatively long ligaments observed in the jet isused from larger length/diameter ratio nozzle are an indication of a significant interaction with the ambient (cross airflow). These observations imply that the liquid jet is turbulent. The influence of the exit conditions of a fully developed turbulent flow on the liquid jet trajectory in the far-field region (up to $z_b/d_j \approx 80$) for both small and large length/diameter ratio nozzles is qualitatively shown in Fig. 5c and d. As depicted in Fig. 5d, the turbulent jet exhibits an active and unsteady breakup process with a shorter breakup length, and it also bends into the crossflow slightly more than the nonturbulent jet (Fig. 5c). Hence, it appears that the disturbance of the jet, caused by turbulence, is an important factor for liquid column breakup in addition to the aerodynamic force of the crossflow. These qualitative observations will be quantified in the following sections.

In order to support the aforementioned observations, PIV velocity measurements in the near-field region of the liquid jet injected into a quiescent atmosphere are acquired at several axial planes; i.e., $z = 2, 10$ and 20 mm. Figure 6 shows the radial profiles of the liquid jet axial mean velocity and its corresponding turbulence intensity for different nozzles at three axial planes. It is observed that the axial mean velocity increases in the flow directions farther away from the nozzle exit (from the plane $z = 2$ to $z = 20$ mm), as shown in Fig. 6a, c, and e. These figures also show that the nozzles with the larger length/diameter ratio (N (4) and N (2)) tend to produce flatter velocity profiles indicating that the issuing liquid jet is turbulent. In addition, the higher turbulence intensity of the nozzles with the larger length/diameter ratio (Fig. 6a, c and e), along with a lower mean velocity profiles (Fig. 6b,
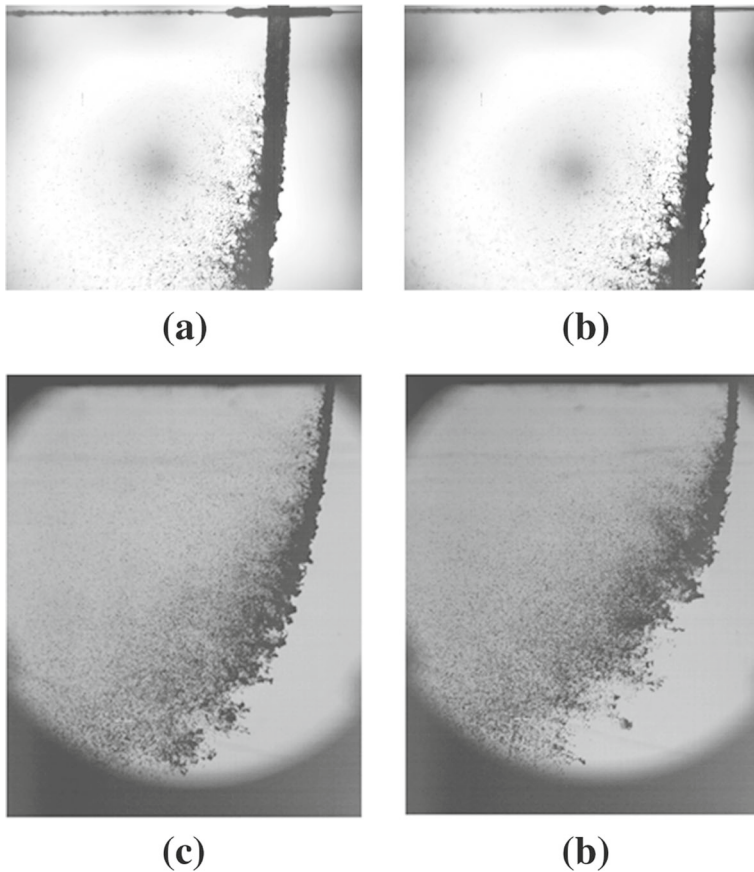
Fig. 5 Flow visualization showing the effect of turbulent nozzle exit conditions on water jet for $v_j = 21$ m/s, $Re_j = 39965$, $q = 87$, and $We_g = 134$; where (**a**) $L/d_j = 4/d_j \approx 12$), (**b**) $L/d_j = 40$ (up to $z_b/d_j \approx 12$), (**c**) $L/d_j = 4$ (up to $z_b/d_j \approx 80$), (**d**) $L/d_j = 40$ (up to $z_b/d_j \approx 80$)

d and f), suggest a faster disruption of the liquid column surface and consequently a shorter column breakup length (see Fig. 5d).

In order to quantitatively assess the effect of nozzle exit turbulence on the liquid jet trajectory and its breakup location, the effect nozzle geometry was first investigated by determining the discharge coefficients of each set of nozzles using Eq. 1. Based on the obtained values of C_d at different range of q, Eq. 6 is then used to find the column breakup height of the transverse jet for different nozzle geometries.

3.2 Liquid jet trajectory

The main focus of this section is to examine the effect of nozzle's turbulent exit conditions on the trajectory of a transverse water jet. This is achieved using small and large L/d_j nozzles when keeping all other non-dimensional controlling parameters constant (e.g., q and We_g). The predicted liquid jet trajectory using Eq. 1 with an unknown discharge coefficient, C_d, is compared with their counterpart's experimental data in order to find the
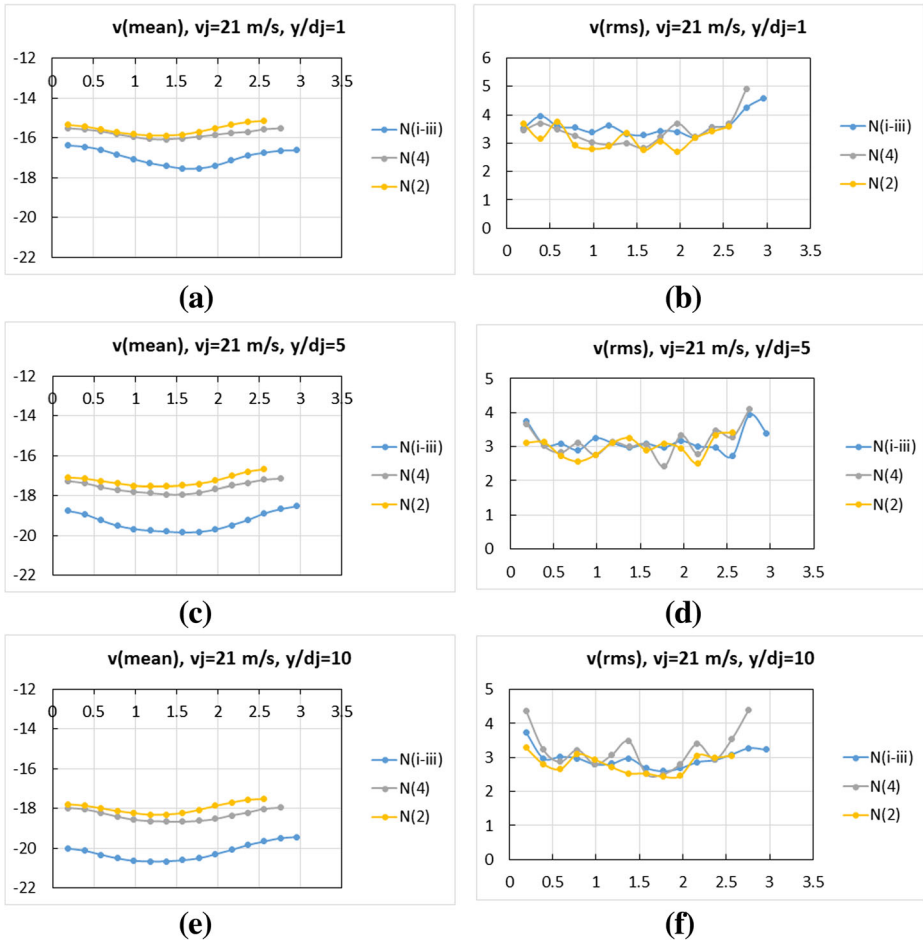
Fig. 6 Radial profiles of axial mean velocity of water jet injected into a quiescent atmosphere for $v_j = 21$ m/s at $z/d_j = 1$, 5 and 10. (**a**, **c** and **e**) axial mean velocity, and (**b**, **d** and **f**) axial intensity

C_d of each nozzle over the tested range of water jet velocity (between 9 and 30 m/s) and two cross airflow velocities (47 and 65 m/s) at standard temperature and pressure (STP) test conditions.

Figure 7 depicts the near-field experimental data of water jet trajectory for different nozzle geometries; namely N (i-iii), N (4) and N (2), under shear breakup regime conditions ($We_g = 134$). The other test conditions consists of $u_g = 65$ m/s, and $v_j = 12$, 21 and 30 m/s. As is expected, the jet penetrates farther with increasing q (see Fig. 7a to c). Furthermore, the trend exihibited in these figures reveals that the jet injected from small L/d_j nozzle (N (i-iii)) penetrates farther than that from large L/d_j nozzles (N (4) and N (2)), particularly when the jet velocity increases (Fig. 7c). This is an indication of the fact that the jet with turbulent exit conditions bends slightly more than the nonturbulent one.
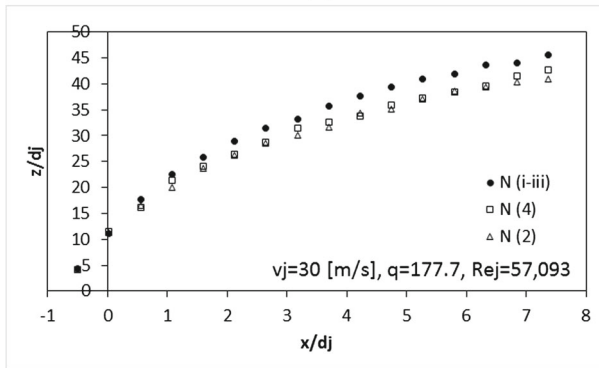
Figure 8 depicts the near-field experimental data of water jet trajectory for nozzles N (i-iii), N (4) and N (2) under multi-mode breakup regime conditions ($We_g = 70$). The test conditions consists of $u_g = 47$ m/s, and $v_j = 12$ (Fig. 8a), 21 (Fig. 8b), and 30 m/s (Fig. 8c).
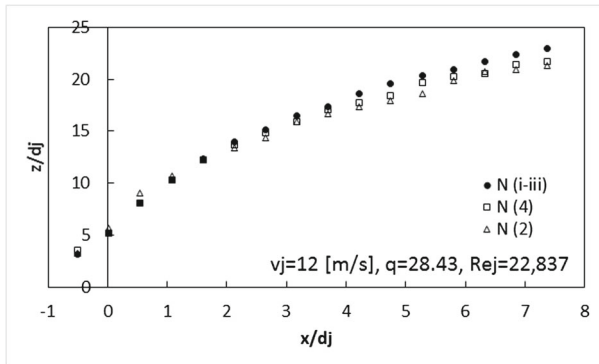
(a)
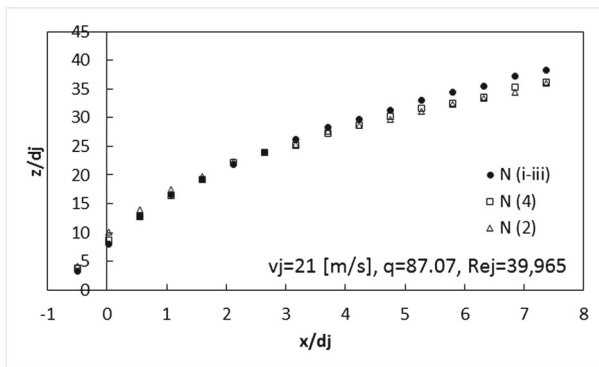
(b)

(c)

Fig. 7 Water jet trajectory for different nozzle geometries in a subsonic crossflow at $We_g = 134$; (**a**) $v_j = 12$, $q = 28$, $Re_j = 22837$, (**b**) $v_j = 21$, $q = 87$, $Re_j = 39965$, and (**c**) $v_j = 30$, $q = 178$, $Re_j = 57093$

Similar to the shear breakup regime conditions (Fig. 7), the nonturbulent liquid jet (nozzle N (i-iii)) in multi-mode breakup regime conditions (Fig. 8a–c) penetrates farther than the turbulent jet.

Jet trajectory predicted by Eq. 1, with unknown C_d, is used to estimate the value of C_d that is capable of reproducing the experimental data. As is shown in Fig. 9, different ranges
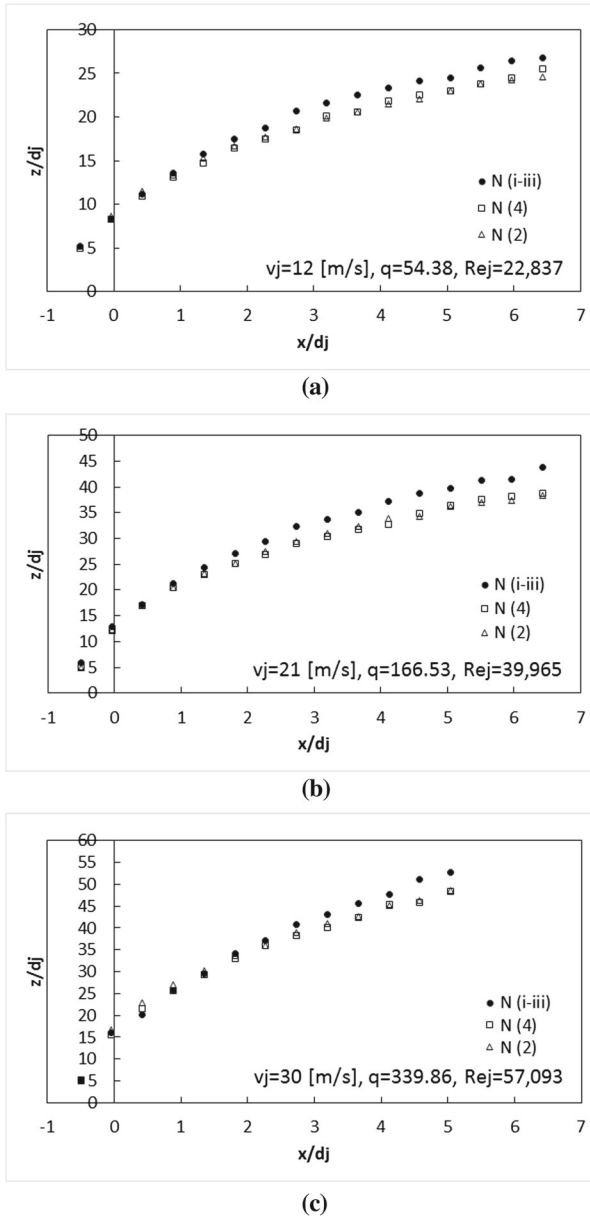
(a)

(b)

(c)

Fig. 8 Trajectory of water jet for different nozzle geometries at $We_g = 70$; (**a**) $v_j = 12$, $q = 54$, $Re_j = 22837$, (**b**) $v_j = 21$, $q = 166$, $Re_j = 39965$, and (**c**) $v_j = 30$, $q = 340$, $Re_j = 57093$

of C_d are calculated for different L/d_j and q. In essence, the discharge coefficient of a plain-orifice nozzle/injector is influenced by different factors such as the nozzle/injector internal geometry, liquid injection pressure, Re_j, turbulence, cavitation and hydraulic flip, and ambient pressure [16]. In this study, as the liquid jet is injected into a cross airflow, instead of a quiescent atmosphere, and in order to take into account the local pressure at the

nozzle's outlet, as well as considering the thickness of the thin non-uniform boundary layer near the wall of the test section, q (i.e., which is a ratio of liquid inertia to gas inertia) is used to plot C_d in Fig. 9. As is illustrated in this figure, while the value of C_d shows nearly the same increasing trend with q for all examined nozzle geometries at different We_g, C_d is larger for the large L/d_j nozzles (N (4) and N (2)) compared with that of the small L/d_j nozzle (N(i-iii)). This demonstrates the importance of considering the influence of turbulent liquid jet exit conditions (i.e., which can be represented by nozzle's discharge coefficient, C_d) on the liquid jet trajectory.

3.3 Liquid jet breakup length

To show the effect of turbulence at the nozzle exit, which is represented by the nozzle's discharge coefficient, on the column breakup height of a transverse liquid jet, the breakup location is calculated using Eq. 6 while taking into account the discharge coefficient of each nozzle for each corresponding q and We_g from Fig. 9. The computed breakup location is compared with its counterparts' experimental data obtained in the present study. The column breakup height obtained from the present correlation and that from the experiments are also compared with published correlations (Thawley et al. [37]). As is shown in Fig. 10, the calculated height (using Eq. 6) shows a good agreement with the present experimental data, while the correlation from Thawley et al. [37] with a constant coefficient $(z_b/d_j = 2.5q^{0.53})$ overestimates the present experimental results at high values of q. This is again an illustration of the importance of considering the nozzle's turbulent exit conditions; that is, the nozzle's discharge coefficient, in determining the column breakup height.

Figure 11 presents a comparison of the water column's breakup height, z_b/d_j, for different nozzle geometries obtained from Eq. 6. It is evident that the column breakup height of the water jet injected from a shorter L/d_j nozzle (N (i-iii)) is higher than the breakup height of the larger L/d_j. This is in agreement with the literature where, for instance, Ahn et al. [20], Lee et al. [22], and Osta et al. [23], stated that the presence of turbulence enhances the process of liquid column breakup as a whole, and consequently shortens the column breakup time and length of a turbulent liquid jet in a crossflow when compared with a nonturbulent
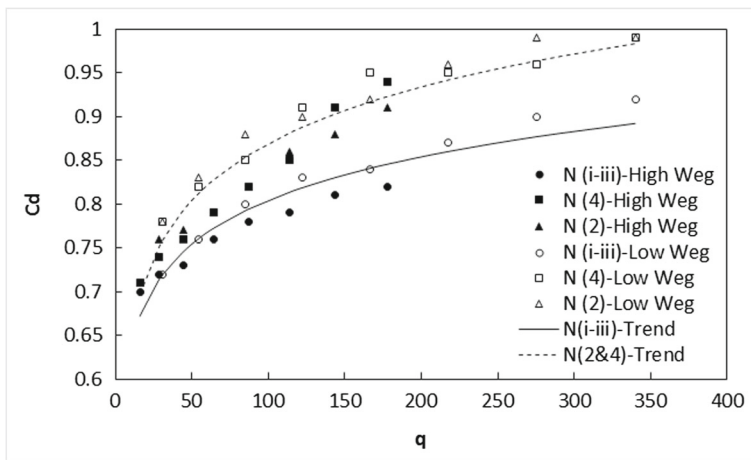

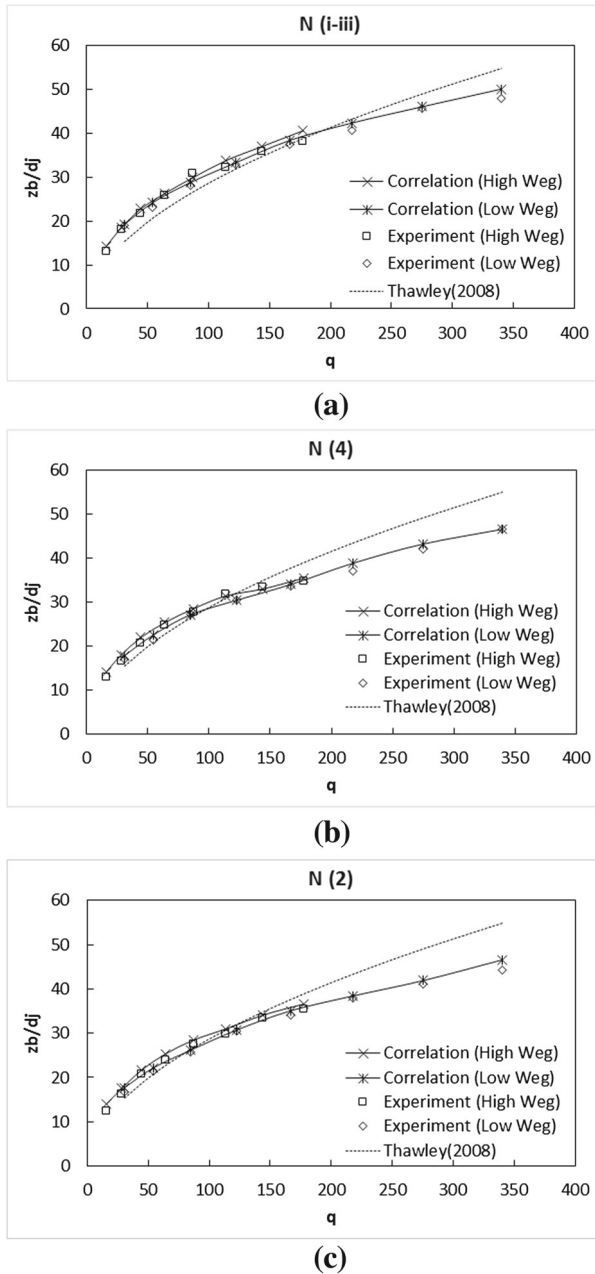**Fig. 9** Discharge coefficient for various nozzle geometries at different We_g as a function of q

Fig. 10 Water column's breakup height in a subsonic crossflow for various values of We_g as a function of q for (**a**) nozzle N (i-iii), (**b**) nozzle N (4), and (**c**) nozzle N (2)

liquid jet. In essence, according to Lefebvre [16], for a fully turbulent jet, the radial velocity component soon causes disruption of the surface film, and consequently the precipitation of the disintegration of the jet.
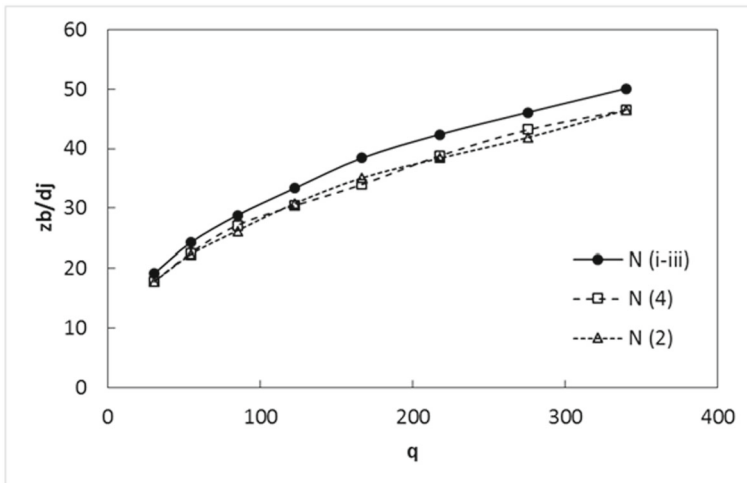
Fig. 11 Comparison of water column's breakup height of different nozzle geometries

The measurements suggest that the column breakup distance, x_b/d_j, overall remaines constant for different nozzle internal geometry, and q. In the present study, the column breakup distance occurs in the range of $C_x = 5.69$ to 7.01 jet diameters downstream of the nozzle, which is in the range that Osta et al. [23] reported for the column breakup distance using different nozzle geometries, that is $x_b/d_j = 5.20$ to 8.

4 Conclusions

The effect of nozzle internal geometry on the ensuing liquid jet turbulence at the nozzle exit, as well as its impact on the trajectory and column breakup location of a transverse liquid jet, are investigated at different test conditions. The results show a higher penetration and breakup height for a nonturbulent liquid jet compared to a turbulent jet. This is attributed to the surface irregularities produced by turbulent structures along a liquid column of a turbulent liquid jet which causes the jet to break up and follow the cross airflow sooner. It is shown that since both the jet trajectory and column breakup height are directly proportional to q, accounting for C_d in determining v_j is critical. In this regard, two modified correlations for predicting a tranverse liquid jet trajectory and its breakup height are proposed which take into account the discharge coefficient. The discharge coefficient is first found through a comparison of the analytically predicted trajectory with its experimental counterpart, and the estimated coefficients are employed in the analytical correlation in order to render it possible to prectict the breakup characteristics of both turbulent and non-turbulent transverse liquid jet. Overall, it is concluded that to reach a more comprehensive correlations for predicting a transverse liquid jet's trajectory and column breakup location, the effect of nozzle length to diameter ratio on jet's exit turbulence conditions should be taken into account via, for example, the discharge coefficient of a nozzle. Therefore, in order to expand the validity of the proposed correlation, the effect of the discharge coefficient of other types of nozzles (such as sharp-edge nozzle) should be determined. The generalization of these correlations requires further testing to include elevated temperature and pressure (HTP) test conditions.

Compliance with Ethical Standards

Conflict of Interest   The authors declare that they have no conflict of interest.

References

1. Ashgriz, N.: Handbook of Atomization and Sprays. Springer Science Business Media LLC, pp 657–683 (2011)
2. Karagozian, A.R.: Transverse jets and their control. Prog. Energy Combust. Sci. **36**(5), 531–553 (2010)
3. Desantes, J.M., Arrègle, J., López, J.J., García, J.M.: Turbulent gas jets and diesel-like sprays in a crossflow: A study on axis deflection and air entrainment. Fuel **85**(14–15), 2120–2132 (2006)
4. Padala, S., Le, M.K., Kook, S., Hawkes, E.R.: Imaging diagnostics of ethanol port fuel injection sprays for automobile engine applications. Appl. Therm. Eng. **52**(1), 24–37 (2013)
5. Birouk, M., Azzopardi, B.J., Stäbler, T.: Primary Break-up of a Viscous Liquid Jet in a Cross Airflow. Part. Part. Syst. Charact. **20**(4), 283–289 (2003)
6. Birouk, M., Stäbler, T., Azzopardi, B.J.: An experimental study of liquid jets interacting with cross airflows. Part. Part. Syst. Charact. **20**, 39–46 (2003)
7. Jadidi, M., Moghtadernejad, S., Dolatabadi, A.: Penetration and breakup of liquid jet in transverse free air jet with application in suspension-solution thermal sprays. Mater. Des. **110**, 425–435 (2016)
8. Schetz, J.A., Padhye, A.: Penetration and breakup of liquids in subsonic airstreams. AIAA J. **15**(10), 1385–1390 (1977)
9. Wu, P.-K., Kirkendall, K.A., Fuller, R.P., Nejad, A.S.: Breakup processes of liquid jets in subsonic crossflows. J. Propuls. Power **13**(1), 64–73 (1997)
10. Behzad, M., Ashgriz, N., Mashayek, A.: Azimuthal shear instability of a liquid jet injected into a gaseous cross-flow. J. Fluid Mech. **767**, 146–172 (2015)
11. Linne, M.: Imaging in the optically dense regions of a spray: A review of developing techniques. Prog. Energy Combust. Sci. **39**(5), 403–440 (2013)
12. Sedarsky, D., Paciaroni, M., Zelina, J., Linne, M.: Near field fluid structure analysis for jets in crossflow with ballistic imaging. In: ILASS Americas 20th Annual Conference on Liquid Atomization and Spray Systems (2007)
13. Wang, M., Broumand, M., Birouk, M.: Liquid Jet Trajectory in a Subsonic Gaseous Cross-flow: an Analysis of Published Correlations. At. Sprays **26**(11), 1083–1110 (2016)
14. Broumand, M., Birouk, M.: Liquid jet in a subsonic gaseous crossflow: Recent progress and remaining challenges. Prog. Energy Combust. Sci. **57**, 1–29 (2016)
15. Brown, C., McDonell, V.: Near field behavior of a Liquid Jet in a Crossflow. In: ILASS Americas (2006)
16. Lefebvre, A.H.: Atomization and Sprays. Hemisphere, New York (1989)
17. Brown, C.T., Mondragon, M.U., McDonell, G.V.: Investigation of the Effect of Injector Discharge Coefficient on Penetration of a Plain Liquid Jet into a Subsonic Crossflow. In: ILASS Americas 20th Annual Conference on Liquid Atomization and Spray Systems, pp. 15–18 (2007)
18. Brown, C.T., Mondragon, U.M., McDonell, V.G.: Liquid Jet in Crossflow: Consideration of Injector Geometry and Liquid Physical Properties. In: ILASS Americas 25th Annual Conference on Liquid Atomization and Spray Systems (2013)
19. Ahn, K., Kim, J., Yoon, Y.: Effect of Cavitation on Transverse Injection into Subsonic Crossflows. In: 39th AIAA/ASME/SAE/ASEE Joint Propulsion Conference and Exhibit American Institute of Aeronautics and Astronautics (2003)
20. Ahn, K., Kim, J., Yoon, Y.: Effects of orifice internal flow on transverse injection into subsonic crossflows: Cavitation and hydraulic flip. At. Sprays **16**(1), 15–34 (2006)
21. Lubarsky, E., Shcherbik, D., Bibik, O., Gopala, Y., Bennewitz, J.W., Zinn, B.T.: Fuel Jet in Cross Flow-Experimental Study of Spray Characteristics. In: 23rd Annual Conference on Liquid Atomization and Spray Systems (2011)
22. Lee, K., Aalburg, C., Diez, F.J., Faeth, G.M., Sallam, K.A.: Primary breakup of turbulent round liquid jets in uniform crossflows. AIAA J. **45**(8), 1907–1916 (2007)

23. Osta, A.R., Sallam, K.A.: Nozzle-Geometry Effects on Upwind-Surface properties of turbulent liquid jets in gaseous crossflow. J. Propuls. Power **26**(5), 936–946 (2010)
24. Sallam, K.A., Aalburg, C., Faeth, G.M.: Breakup of round nonturbulent liquid jets in gaseous crossflow. AIAA J. **42**(12), 2529–2540 (2004)
25. Wu, P.-K., Miranda, R.F., Faeth, G.M.: Effects of initial flow conditions on primary breakup of nonturbulent and turbulent round liquid jets. At. Sprays **5**(2), 175–196 (1995)
26. Farvardin, E., Johnson, M., Alaee, H., Martinez, A., Dolatabadi, A.: Comparative study of biodiesel and diesel jets in gaseous crossflow. J. Propuls. Power **29**(6), 1292–1302 (2013)
27. Eslamian, M., Amighi, A., Ashgriz, N.: Atomization of liquid jet in High-Pressure and High-Temperature subsonic crossflow. AIAA J. **52**(7), 1374–1385 (2014)
28. Broumand, M., Birouk, M.: A model for predicting the trajectory of a liquid jet in a subsonic gaseous crossflow. At. Sprays **25**(10), 871–893 (2015)
29. Broumand, M., Birouk, M.: Two-Zone Model for predicting the trajectory of liquid jet in gaseous crossflow. AIAA J. **54**(5), 1499–1511 (2016)
30. Sallam, K.A., Dai, Z., Faeth, G.M.: Liquid breakup at the surface of turbulent round liquid jets in still gases. Int. J. Multiph. Flow **28**(3), 427–449 (2002)
31. Iyogun, C.O., Birouk, M., Popplewell, N.: Trajectory of water jet exposed to low subsonic Cross-Flow. At. Sprays **16**(8), 963–980 (2006)
32. Birouk, M., Iyogun, C.O., Popplewell, N.: Role of viscosity on trajectory of liquid jets in a Cross-Airflow. At. Sprays **17**(3), 267–287 (2007)
33. Birouk, M., Baafour, N.-K., Popplewell, N.: Effect of nozzle geometry on breakup length and trajectory of liquid jet in subsonic crossflow. At. Sprays **21**(10), 847–865 (2011)
34. Iyogun, C.O.: Trajectory of liquid jets exposed to a low subsonic cross airflow. University of Manitoba, M.Sc.Thesis (2005)
35. Baafour, N.-K.: Experimental examination of nozzle geometry on water jet in a subsonic crossflow. University of Manitoba, M.Sc.Thesis (2011)
36. Stenzler, J.N., Lee, J.G., Santavicca, D.A., Lee, W.: Penetration of liquid jets in a Cross-Flow. At. Sprays **16**(8), 887–906 (2006)
37. Thawley, S.M., Mondragon, U.M., Brown, C.T., Mcdonell, V.G.: Evaluation of Column Breakpoint and Trajectory for a Plain Liquid Jet Injected into a Crossflow, 1–11 (2008)